X-Ray Peak Broadening Analysis in Fe₃O₄ Nano-Particles

Ahmad Gholizadeh

School of Physics, Damghan University (DU), Damghan, I.R. Iran

Abstract

In this work, structural properties of Fe_3O_4 compound prepared by co-precipitation technique and annealed in presence of oxygen at 200°C is investigated. The structural characterization of Fe_3O_4 nano-particles using X'pert package and Fullprof program is evidence for a cubic structure (F d-3m space group). This result has been confirmed by FTIR measurement. In addition, a comparative study of the crystallite size of the compounds obtained from powder XRD is reported. the Williamson-Hall analysis, size-strain plot and Halder-Wagner methods were used to study the individual contributions of crystallite sizes and lattice micro-strain on isotropic line broadening of all the reflection peaks of the Fe_3O_4 compound and the crystallite sizes results are compared with the Scherer and TEM methods. The Results show the H-W method is more accurate, with all data points touching the fitting line better than the other methods. Also, the crystallite size D_{H-W} is different to the particle size D_{TEM} due to the irregular shape of nanoparticles.

Keywords: Fe_3O_4; Cubic spinel structure; Crystallite sizes; Lattice micro-strain; Isotropic line broadening.

1. Introduction

Both of preparation technique and the crystal imperfections can affect the properties of nanostructures. Bragg's equation assumes crystal is perfect and infinite and incident beam is perfectly parallel and monochromatic. Actual experimental conditions are different from these leading various kinds of deviations from Bragg's condition. Peaks are not 'δ' curves and peaks are broadened. There are also deviations from the assumptions involved in the generating powder patterns. For example, in a powder sample if the crystallite size be smaller than 0.5 μm, there are insufficient number of planes to build up a sharp diffraction pattern and then peaks are broadened.

The half width of the experimentally measured breadth (β) can be influenced by instrumental (β_I), crystallite size (β_C), lattice microstrain (β_S), stacking fault (β_{SF}) and other defects. Consequently:

$$\beta(FWHM) = \beta_I + \beta_C + \beta_S + \beta_{SF} + \ldots \tag{1}$$

Full Width at Half-Maximum (FWHM) is typically used as a measure of the peak 'width'. The instrumental broadening are originated from unresolved α_1, α_2 peaks, non-monochromaticity of the source (finite width of α peak) and imperfect focusing. An ideal crystal would extend infinitely in all directions; therefore, no crystals are perfect due to their finite size. The effect of this deviation from perfect crystallinity changes the broadening of diffraction peaks. Therefore, in the vicinity of θ_B the Bragg's equation not being satisfied that it led to crystallite size broadening. 'Residual Microstrain' arising from dislocations, coherent precipitates etc. leading to lattice microstrain broadening. Lattice strain is a measure of the distribution of lattice constants arising from crystal imperfections, such as lattice dislocations due to different ionic radii of dopants comparing to the matrix ions. In principle, every defect contributes to some broadening. The diffraction peak we see is a result of various broadening 'mechanisms' as shown in Fig. 1.
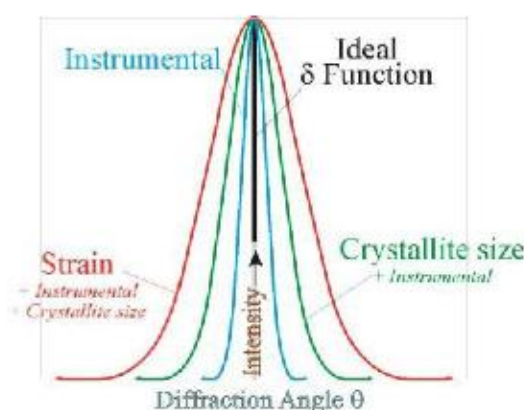
Fig. 1: The contribution of the instrumental (β_I), the crystallite size (β_C), the lattice microstrain (β_S) broadening on diffraction peak.

The β_I is determined using the undeformed aluminum or silicon as a standard reference material by diffractometer. However, instrumental broadening has to be subtracted to get the broadening effects due to the sample and consequently Eq. 1 is rewritten as follow:

$$\beta_{hkl} = \beta - \beta_I = \beta_C + \beta_S + \beta_{SF} + \ldots \tag{2}$$

The peaks are fitted to various profiles. For a peak with a Lorentzian profile:

$$\beta - \beta_I \approx \beta_C - \beta_S = \beta_{hkl} \tag{3}$$

For a peak with a Gaussian profile:

$$\beta_{hkl}^2 = \beta^2 - \beta_I^2 \tag{4}$$

A geometric mean can also used:

$$\beta_{hkl}^2 = (\beta - \beta_I)\sqrt{\beta^2 - \beta_I^2} \tag{5}$$

Both crystallite size and lattice microstrain have effects on Bragg peaks by increasing the peak width, intensity and shifting the 2θ peak position (Fig. 2).

In this paper, we analyzed XRD data of Fe_3O_4 prepared by co-precipitation technique using a commercial X'pert package and Fullprof program and tried to explain the structural properties. In addition, a comparative study of the mean crystallite size of the compounds obtained from powder XRD is reported. The microstrain due to lattice deformation of Fe_3O_4 nanoparticles was estimated by Williamson-Hall (W-H) analysis, size-strain plot (SSP) and Halder-Wagner (H-W) methods and the crystallite sizes results obtained by these methods are compared with the Scherer and TEM methods.

2.   Experimental

2.1   Sample synthesis

the Fe_3O_4 nano-particles were prepared according to following method. $FeCl_2 \cdot 4H_2O$ (0.01 mol) and $FeCl_3 \cdot 6H_2O$ (0.02 mol) were dissolved in 120 mL deionized water, and then, 60 mL $NH_3 \cdot H_2O$ was added under vigorous mechanical stirring. The color of the suspension turned black immediately. Afterward, the mixture was kept at 70°C for 30 min. The mechanical stirring was carried out

throughout the reaction. After cooling down, the precipitated powders were collected by magnetic separation and washed with deionized water.
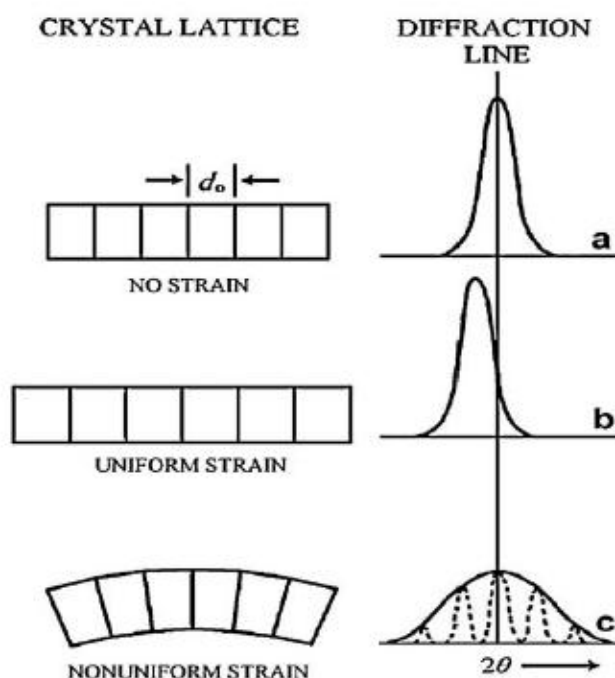

Fig. 2: A portion of an unstrained grain appears in (a), uniform tensile strain (b) and nonuniform strain (c). According to the figure the uniform strain affect the peak position and the nonuniform strain affect the peak broadening and intensity [Khorsand Zak et al., 2011].

2.2 Geometric characterization

XRD, and TEM were used to obtain the textural parameters of the materials, such as size, shape, composition and crystal structure. The X-ray diffraction (XRD) pattern has been recorded using a Bruker AXS diffractometer D8 ADVANCE with Cu-Kα radiation in the range $2\theta = 20\text{-}80°$ at room temperature (RT). The XRD data was analyzed using a commercial X'pert package and Fullprof program.

XRD profile analysis is a simple and powerful method to evaluate the crystallite size and lattice microstrain. Two factors determine the breadth of Bragg's peak including crystallite size-dependent (β_C) and microstrain dependent broadening (β_S) effects, except instrument-dependent effect. To do an accurate analysis for size and microstrain effects, at first, Instrumental broadening has to be subtracted using the undeformed silicon as a standard reference material to get the broadening effects due to the sample.

The FT-IR spectra of samples were recorded in a Perkin-Elmer FT-IR spectrometer in the wave number range of 350-2000 cm^{-1}. The particle size of the samples was investigated by the TEM (LEO Model 912AB) analysis.

3. Results and Discussions

3.1 XRD analysis

are shown in Fig. 3. The XRD data were analyzed using both the commercial X'pert High Score package and Fullprof program. Identification of structure type using X'pert package confirms cubic structure in all sample without the presence of impure phases. The XRD pattern of the sample fits with the diffraction pattern of a cubic structure Fe_3O_4 (JCPDS, 74-2399). Results of the Rietveld analysis using Fullprof program indicate that all the diffraction peaks of the XRD pattern for the sample can be quite well indexed to the cubic structure (Fd-3m space group) as shown in Fig. 3. To perform a Rietveld refinement good initial values for lattice parameter is needed. The type of space group is obtained from phase analysis of X'pert package. The derived lattice parameter of the sample is 8.409 Å.
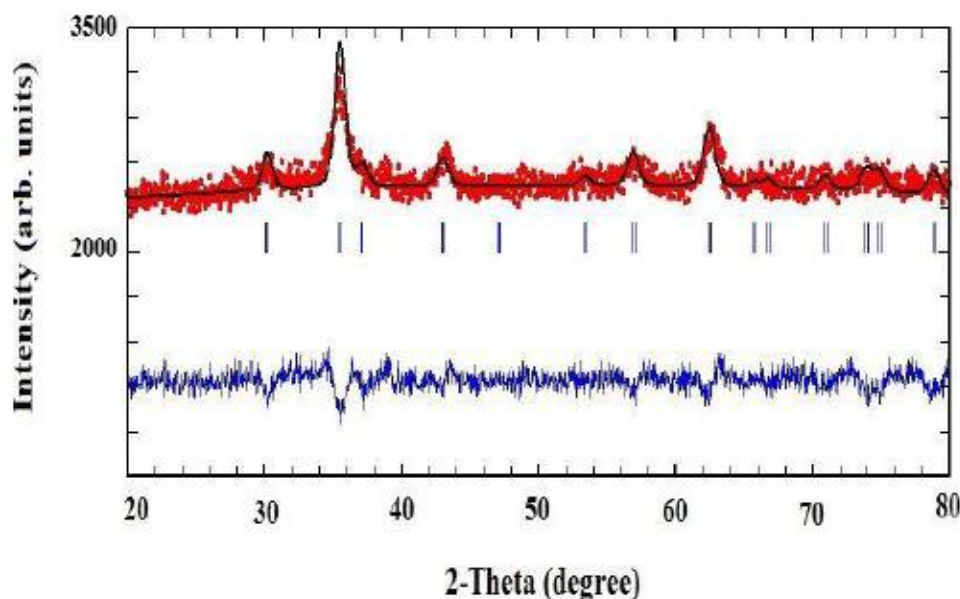

Fig. 3: Rietveld analysis of the XRD pattern for Fe_3O_4. The circle signs represent the raw data. The solid line represents the calculated profile. Vertical bars indicate the position of Bragg's peaks for the cubic structure (Fd-3m Space Group). The lowest curve is the difference between the observed and the calculated pattern.

Fig. 4 shows the IR spectra of Fe_3O_4 nanoparticles. The positions of two strong bands v_1 and v_2 around 600 cm^{-1} and 400 cm^{-1} are related to Cubic spinel phase. The band v_1 is assigned to the vibrations of the bond between the tetrahedral metal ion and the oxygen ion M_{tetra}– O. Also, the band v_2 is assigned to the vibrations of the bond between the octahedral metal ion and the oxygen ion M_{octa}– O. Therefore, the formation of spinel structure obtained from XRD result has been confirmed by FTIR measurement.
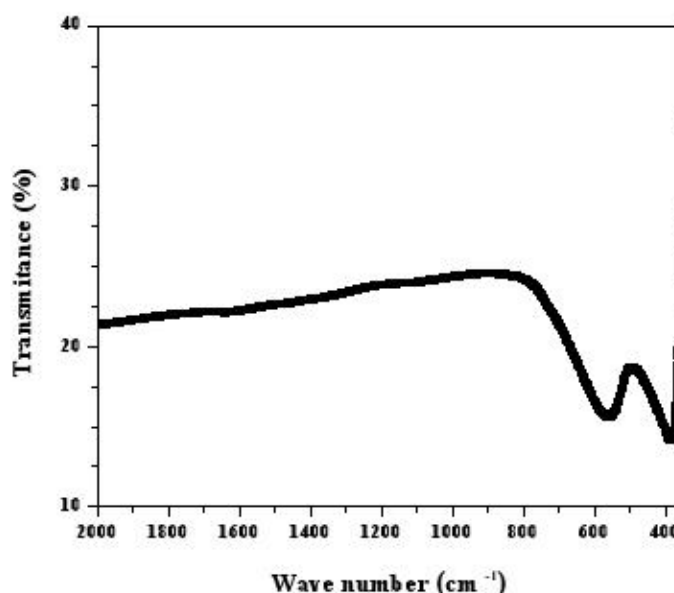
٤

Fig. 4: FT-IR spectra for Fe₃O₄.

3.2 Determination of crystallite size, microstrain and particle size

In below, a comparative study of the mean crystallite size of Fe_3O_4 obtained from powder XRD is reported. The microstrain due to lattice deformation of Fe_3O_4 nanoparticles was estimated by W-H, SSP and H-W methods and the crystallite sizes results obtained by these methods are compared with the Scherer, magnetic and TEM methods. In all the methods, the values of β_{hkl} (the full-width at half-maximum (FWHM) of the diffraction peaks) and θ are selected from result obtained of rietveld refinement using Fullprof program corresponding to the 7 strongest peaks of Fe_3O_4 shown in Fig. 3. Also, the values of d_{hkl} (the distance between adjacent planes in the Miller indices (hkl)) are calculated ⬚ h⬚⬚sin⬚$=$⬚, with $\lambda = 1.5404$ Å.

3.2.1 Scherrer method

The instrumental corrected broadening [Rogers and Daniels, 2002] β_{hkl} ($= \beta_C$) was estimated by using Gaussian function:

$$\beta_C^2 = \beta_{hkl}^2 = \beta^2 - \beta_I^2 \tag{6}$$

Also, Scherrer's equation as follows:

$$⬚h⬚⬚=⬚⬚⬚\ cos⬚=⬚⬚ \tag{7}$$

show the broadening of the XRD pattern which is attributed to the crystallite size-induced broadening. Here, β_{hkl} is the full-width at half maximum (FWHM) corresponding to the 7 strongest peaks of Fe_3O_4 shown in Fig. 3, K is the Scherrer constant equal to 0.94, D is the crystallite size, λ the wavelength of the X-ray, and θ is the Bragg's angle.

o

In this method, increase of peak broadening is due to decrease of crystallite size. The Scherrer's formula is used for the determination of crystallite size from Gaussian line profiles. The formula is not expected to be valid for very small crystallite sizes (<10 nm).

In Scherrer method, plot was drawn with $1/\beta_{hkl}$ on the x-axis and $cos\theta$ along the y- axis. By fitting the data, the crystallite size (D) of Fe_3O_4 was extracted from the slope of the fit line.

3.2.2   Williamson-Hall method

In the W-H method, the information on microstrain (ε) and the crystallite size (D) of Fe_3O_4 have been obtained from β_{hkl} by using W-H relation. Microstrain broadening in W-H method is defined as follows [Stokes and Wilson, 1944]:

$$\varepsilon = 4\varepsilon \tan\theta \tag{8}$$

Separating crystallite size broadening and microstrain broadening:

$$\beta_{hkl} = \beta_C + \beta_S = \frac{K\,\lambda}{D\cos\theta} + 4\varepsilon\,tan\,\theta \tag{9}$$

Rewriting Eq. (9), Formula for Williamson-Hall method is as follow [Williamson and Hall, 1953]:

$$\beta\,/\cos\theta = \lambda\,/\,D + (4\varepsilon\,\sin\,\theta) \tag{10}$$

where K is the Scherrer constant or the shape coefficient given as 0.94 for spherical particles and ε is the internal microstrain.

$\beta\,/\cos\theta$ (axis-y) versus $4\sin\theta$ (axis-x) corresponding to the 7 strongest peaks of Fe_3O_4 shown in Fig. 3, is straight line. The slope and intercept of linearly fitted data give amounts of micro-strain (ε) and crystallite size D_{W-H} respectively.

The negative microstrain obtained may be caused by the lattice contraction. Basically, the larger the intercept result the smaller the crystallite size and the larger the slope result the larger the microstrain. Intercept with origin means D is infinity or broadening is only due to microstrain broadening and zero slope means horizontal line with no microstrain or broadening is only due to crystallite size broadening. The value of D_{W-H} is not true due to very low value of R^2.

3.2.3   size-strain plot method

The information on microstrain (ε) and the crystallite size (D) of Fe_3O_4 have been obtained from β_{hkl} and planar spacing d_{hkl} (the distance between adjacent planes in the set ($h\,k\,l$)) by using size-strain plot (SSP) method. The SSP method is more accurate, especially at higher diffraction angles. Therefore, the crystallite size and lattice strain of the sample was calculated using the size-strain plot (SSP) $\beta\,tan\theta$ [Cullity, 1956]. Therefore, the total broadening is obtained from:

$$\beta\,/\cos\theta = \lambda\lambda + \varepsilon\varepsilon \tag{11}$$

According to the SSP method, the relation between lattice strain and crystallite size is given by [Tagliente and Massaro, 2008]:

$$(\beta\,/\cos\theta\,/\,\lambda\,/\,d^2\cos\theta)2 = \lambda\,/\lambda\,/\beta\,2\varepsilon\,/\,d^2\cos\theta + (\lambda/2)2 \tag{12}$$

where K is the shape coefficient given as 3/4 for spherical particles.

$(\beta\,/\cos\theta\,/\,d^2\cos\theta)2$ (axis y) versus $\beta\,/\,d^2\,2\varepsilon\,/\,d^2\cos\theta$ (axis-x) corresponding to the 7 strongest peaks of Fe_3O_4 shown in Fig. 3, is straight line. The crystallite size is determined from the slope of the linearly fitted data and the root of the y-intercept gives the microstrain.

3.2.4   Halder-Wagner method

The information on microstrain (ε_{H-W}) and the crystallite size (D_{H-W}) of Fe_3O_4 have been obtained from β_{hkl} and planar spacing d_{hkl} (the distance between adjacent planes in the set ($h\,k\,l$)) by using H-W

٦

method. Halder and Wagner have given an approximation to the integral breadth of a Voigt function as [Halder and Wagner, 1966]:

$$\beta_h^2 = \beta_L \beta_h + \beta_G^2 \qquad (13)$$

where β_L and β_G are the Lorentzian and Gaussian components, respectively. In H-W method, the crystallite size and strain profiles are described by the Lorentzian and the Gaussian function, respectively. Consequently, we have [Langford, 1992]:

$$\left(\frac{\beta_h^*}{d_h^*}\right)^2 = \frac{1}{D}\left(\frac{\beta_h^*}{d_h^{*2}}\right) + \frac{\varepsilon}{2}^2 \qquad (14)$$

$\beta_h^* = \beta_h \cos\theta / \lambda$ and $d_h^* = 2\sin\theta / \lambda$.

β_h^*/d_h^{*2} (axis y) versus β_h^*/d_h^{*2} (axis-x) corresponding to the 7 strongest peaks of Fe_3O_4 shown in Fig. 3, is straight line with a positive slope and a nonzero y-intercept. The crystallite size is determined from the slope inverse of the linearly fitted data and the root of the y-intercept gives the microstrain, respectively.

The results of crystallite size and microstrain of Fe_3O_4 estimated by the Scherrer, W-H, SSP and H-W methods are summarized in Table 1. All the methods shows that line broadening were essentially isotropic. W-H method supposes that "crystallite size" profile and the "microstrain" profile contribute to the line broadening with Lorentzian profiles but in both of the S-S and H-W methods are assumed that the "crystallite size" profile is described by a Lorentzian function and the "microstrain" profile by a Gaussian function. However, both of the S-S and H-W methods with respect to Scherrer and W-H methods have the advantage that less weight is given to data from reflections at high angles, where the precision is usually lower. For this reason, in W-H method is suggested that the smaller angle peaks should be used to separate βc and βs.

The values of average crystallite size of Fe_3O_4 obtained from the different models are less similar, implying that the inclusion of microstrain in various forms has a very large effect on the average crystallite size of Fe_3O_4. However, one method is more accurate which the value of R^2 is near 1 or in the other words, data points of x-y are more touching the fitting line. Here, the H-W method is more accurate. Also, this method has minimum of the microstrain.

Table 1: The values of crystallite size and microstrain of Fe_3O_4 obtained from Williamson-Hall (W-H) analysis, size-strain plot (SSP) and Halder-Wagner (H-W) methods and also particle sizes calculated by magnetic and TEM measurements.

D_{sch} (nm)	D_{W-H} (nm)	ε_{W-H} (no unit) $*10^3$	D_{ssp} (nm)	$\varepsilon_{sp}*10^3$ (no unit)	D_{H-W} (nm)	ε_{H-W} (no unit) $*10^3$	D_{TEM} (nm)
9.2	13.4	2.20	8.24	4.54	10.1	0.98	12

3.2.5 Particle size from TEM method

Particle size distribution histograms of Fe_3O_4 obtained from TEM micrographs is fitted by using a log-normal function as follow:

$$P(d) = \frac{1}{D\sigma_d \sqrt{2\pi}} \exp\left\{ -\frac{1}{2\sigma_d^2} \ln^2\left(\frac{D}{D_{TEM}}\right) \right\} \qquad (15)$$

where σ_d is the standard deviation of the diameter and D_{TEM} is the mean diameter obtained from the TEM results. The mean diameter of particle size D_{TEM} calculated by TEM method is 12 nm.

The $D_{W\text{-}H}$ is more than D_{TEM} and this is not true as a particle size is equal or greater than crystallite size. The result is different from the crystallite size ($D_{H\text{-}W}$) obtained from Halder-Wagner method by XRD line profile. The difference is related to the irregular shape of nanoparticles with spherical, spherodial and polygon morphologies which is observed in the TEM micrograph [Frozandeh-Mehr et al., 2012].

4. Conclusion

The structural characterization of Fe_3O_4 prepared by co-precipitation technique is investigated by X-ray powder diffraction and FTIR measurements. The results X'Pert package and Fullprof program on XRD pattern and also analyze of FTIR are evidences for a Fe_3O_4 structure (Fd-3m space group). The results of crystallite size and microstrain of Fe_3O_4 compound estimated by the Scherrer, W-H, SSP and H-W methods show the H-W method is more accurate, with all data points touching the fitting line better than the other methods. Also, the crystallite size $D_{H\text{-}W}$ is smaller than the particle size D_{TEM} due to the irregular shape of nanoparticles with spherical, spherodial and polygon morphology as observed in the TEM micrograph.

5. References

Cullity B. D., 1956. *Elements of X-ray Diffraction*. Addison-Wesley Publishing Company Inc., California.

Frozandeh-Mehr E., Malekzadeh A., Ghiasi M., Gholizadeh A., Mortazavi Y. and Khodadadi A., 2012. Effect of partial substitution of lanthanum by strontium or bismuth on structural features of the lanthanum manganite nanoparticles as a catalyst for carbon monoxide oxidation. *Catal. Commun.*, 28, pp. 32–37.

Halder N. C. and Wagner N. C. J., 1966. Separation of particle size and lattice strain in integral breadth measurements. *Acta Crystallogr.*, 20, pp. 312-320.

Khorsand Zak A., Abd. Majid W.H., Abrishami M.E. and Yousefi R., 2011. X-ray analysis of ZnO nanoparticles by Williamson-Hall and size-strain plot methods. *Solid State Sci.*, 13, pp. 251-256.

Langford J. E., 1992. International Conference Accuracy in Powder Diffraction II, National Institut of Standards and Technology. *Special Publication 846, Gaithersburg, MD, USA*, pp. 145-148.

Rogers K. D. and Daniels P., 2002. An X-ray diffraction study of the effects of heat treatment on bone mineral microstructure. *Biomaterials*, 23(12), pp. 2577-2587.

Stokes A. R. and Wilson A. J. C., 1944. The diffraction of X rays by distorted crystal aggregates – I. *Proc. Phys. Soc.*, 56, pp. 174-186.

Tagliente M. A. and Massaro M., 2008. Strain-driven (002) preferred orientation of ZnO nanoparticles in ion-implanted silica. *Nucl. Instrum. Methods. B*, 266, pp. 1055–1061.

Williamson G. K., Hall W. H., 1953. X-ray line broadening from field aluminum and wolfram. *Acta Metall.*, 1, pp. 22-25.